

## 2700 MHz Polarization Observations of 17 Supernova Remnants

*D. K. Milne<sup>A</sup> and J. R. Dickel<sup>B</sup>*

<sup>A</sup> Division of Radiophysics, CSIRO, P.O. Box 76, Epping, N.S.W. 2121.

<sup>B</sup> Department of Astronomy, University of Illinois at Urbana-Champaign, Urbana, Illinois 61801, U.S.A.

### *Abstract*

Maps are presented of the polarization and total-power emission at 2700 MHz from 17 supernova remnants, including the Monoceros nebula, the Lupus loop and W44. Directions of the magnetic field and values of the rotation measure are deduced for W44 by combining 2700 and 5000 MHz observations.

### **Introduction**

A series of uniform detailed polarization maps at 2700 MHz obtained with the Parkes 64 m telescope has been published for nine supernova remnants (SNRs): IC 443 and Puppis A (Milne 1971*a*), MSH 14–415 (SN 1006 AD) (Milne 1971*b*), Milne 56 (Milne and Dickel 1971), MSH 09–32, 10–53, 14–63, 15–52 and 15–56 (Milne 1972). In this paper we present the results of further observations, with similar measurements on a further 15 galactic radio sources, all believed to be SNRs. More extensive 2700 MHz maps of IC 443 and MSH 10–53 are also presented.

### **Observations**

The observations and reductions followed the methods used by Milne (1972). The receiver and feed system were the same: a 2700 MHz two-channel parametric receiver correlating the signals from two orthogonal probes in a circular waveguide feed. The observing procedure consisted of scanning in declination at approximately half-beamwidth intervals in right ascension. At each right ascension, a total of four scans was made at position angles separated by 45°. The polarization  $E$  vectors were then obtained by combining these scans in the usual way, but so as to make the ratio of the polarization brightness temperature to the full-beam brightness temperature equal to the degree of polarization. The two main instrumental effects observed by Milne (a variation in antenna gain with orientation of the feed, and an effect related to the gradient of the measured brightness distribution and caused by the beam ellipticity and squint) were remeasured and found to be identical with Milne's observations. These instrumental effects, as well as the scale of the full-beam brightness temperature and the beamwidth (8'·4 arc), were measured from scans through Hydra A, for which a flux density of 23 f.u.\* was assumed. Corrections for the two instrumental effects have been made to the present observations. The

\* 1 flux unit (f.u.) =  $10^{-26}$  W m<sup>-2</sup> Hz<sup>-1</sup>.

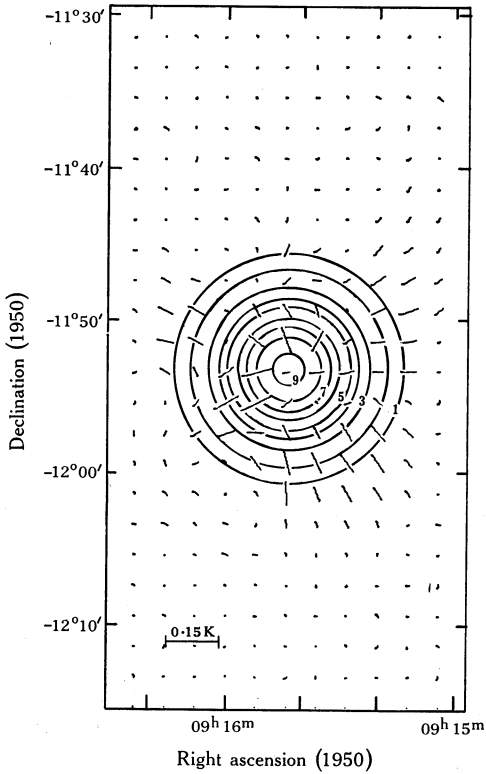


**Fig. 1.** Contours of full-beam brightness temperature and the residual polarization  $E$  vectors at 2700 MHz on Hydra A after correction for the gain and gradient effects. The contour unit is 1.6 K and the  $E$  vector scale is given. Note that the residual polarization is below 0.05% of the peak intensity.

**Table 1.** 2700 MHz flux densities of observed sources

Source	$S_{2700}$ (f.u.)	Source	$S_{2700}$ (f.u.)	Source	$S_{2700}$ (f.u.)
IC 443	$110 \pm 15\%$	Kes 40	$8 \pm 15\%$	Kes 69	$39 \pm 20\%$
0607+17	$13 \pm 15\%$	MSH 17-39	$16.5 \pm 10\%$	G21.5-0.9	$6.8 \pm 10\%$
S34	$13 \pm 15\%$	Kepler's SNR	$9.0 \pm 10\%$	Kes 75	$5 \pm 20\%$
Monoceros neb.	—	W28	$210 \pm 15\%$	NRAO 579	$18 \pm 15\%$
MSH 10-53	—	M20	$11 \pm 10\%$	Milne 62	$34 \pm 20\%$
1156-62	$4.7 \pm 15\%$	A2	$29 \pm 10\%$	W44	$120 \pm 15\%$
Kes 27	$10 \pm 15\%$	PKS 1814-24	$6.3 \pm 15\%$	G35.6-0.0	$12 \pm 20\%$
Lupus loop	$120 \pm 30\%$	Kes 67	$22 \pm 15\%$		

resulting residual (spurious) polarization on Hydra A after applying both corrections is shown in Fig. 1. The indicated scale for the length of the  $E$  vectors corresponds to  $\sim 0.1\%$  of the peak intensity.

For the present observations, an on-line computer was used to drive the telescope, sample the data and perform certain calculations. This permitted the integration of repeated scans to be made at the same position angle for the weaker sources, and therefore the sensitivity is somewhat better than that available to Milne (1972). The stability of the receiver was good, at least over the period of each scan, and we

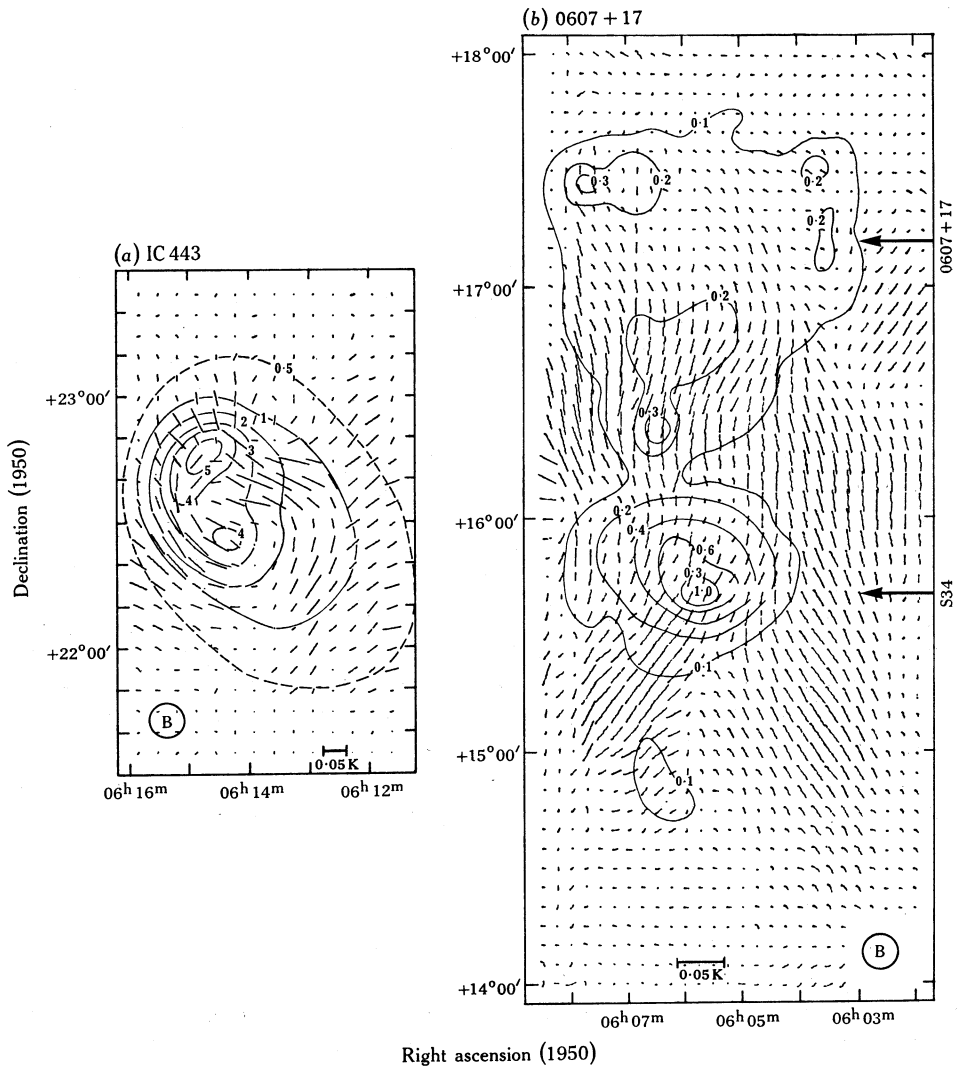


Fig. 2. Total-power contours and polarization  $E$  vectors at 2700 MHz for (a) IC 443 and (b) 0607 + 17. The contour unit is 1.0 K, and the  $E$  vector scale and beam (B) are given.

therefore fitted level linear-baselines to each polarization scan so as to minimize the polarized intensity over those regions of the scan where the total-power brightness temperature was a minimum. In examining the maps (Figs 2–9) presented here this should be borne in mind. Other methods of setting the zero could lead to a different distribution of polarization (with changed position angles). An example of this is to be seen in Kes40 (Fig. 6a), where perhaps a choice of a sloping base level would show polarization associated with the SNR.

The data obtained for each source consist of contours of the total-power brightness distribution and the magnitudes and directions of the polarized intensity over the region. These are presented in Figs 2–9. The total-power contours were integrated for each source, and the deduced integrated flux densities are given in Table 1.

## Discussion

We have also obtained polarization results at 5000 MHz for 11 of the present sources. However, a full discussion of these sources (directions of the magnetic field and the derived Faraday rotation) is reserved for a later paper, and only brief notes are given here on each source.

### *IC 443, G189·1+2·9*

The 2700 MHz polarization observations made on IC 443 by Milne (1971*a*) were incomplete, so we have repeated and extended these observations. The resulting total-power contours and the polarization  $E$  vectors shown in Fig. 2*a* are very similar to those given by Milne, and the polarization is clearly associated with IC 443.

### *0607+17, G193·3-1·5*

The nonthermal source 0607+17 was once identified with the nebula S34 (Davies 1963) but was later shown by Milne and Hill (1969) to be about  $1^\circ$  north of this nebula. The total-power map presented in Fig. 2*b* is of much higher sensitivity than that given by Milne and Hill. It shows an extended region  $1\frac{1}{4}^\circ$  diameter, with some suggestion of peripheral structure centred on R.A.  $06^{\text{h}}06^{\text{m}}30^{\text{s}}$ , Dec.  $+16^\circ 40'$  (1950), which is due north of the prominent source S34. The flux densities measured here for 0607+17 and S34 agree well with the values given by Milne and Hill, but are a factor of two higher than those given by Day *et al.* (1972) at 2700 MHz. The present measurements and those of Milne and Hill show that 0607+17 is nonthermal (spectral index  $\alpha \approx -0.5$ ) and S34 is thermal. The polarization vectors in Fig. 2*b* show several areas of uniform polarization. However, there is no evidence for associating this polarization with 0607+17. No other polarization measurements have been made in this field.

### *Monoceros nebula, G205·5+0·2*

The total-power observations presented here (Fig. 3) are at a slightly higher sensitivity than the Parkes 2700 MHz galactic survey (Day *et al.* 1972) and show weak radio emission associated with the southernmost part of the Monoceros nebula. In other respects the isotherms are very similar to those obtained by Day *et al.* In the present survey we avoided the western side of the Monoceros nebula where it was confused with the Rosette nebula, a bright HII region, and consequently we have not integrated the isotherms for this source. Milne and Hill (1969), Caswell (1970) and Haslam and Salter (1971) have shown that the radio spectrum of the Monoceros nebula is nonthermal, and Lozinskaya (1972) has measured an expansion velocity of  $45 \text{ km s}^{-1}$  for the optical features. It is generally accepted as being an SNR located at  $\sim 600$  pc from the Sun. Only a few small knots of polarization greater than the noise are shown in Fig. 3, and these do not appear to be associated with the Monoceros nebula.

### *MSH 10-53, G284·2-1·8*

The present observations (Fig. 4*a*) cover a much larger region about MSH 10-53 than that mapped by Milne (1972) and include the RCW 48 complex to the north of MSH 10-53. The polarization vectors presented here agree reasonably well

with those given by Milne. However, the present observations show considerable polarization not associated with MSH 10-53. Some of this appears to be in the direction of the thermal source RCW 48 (R.A.  $10^{\text{h}} 18^{\text{m}}$ , Dec.  $-57^{\circ} 45'$ ) and there are other brightly polarized regions which must be due to the polarization of the general galactic background emission.

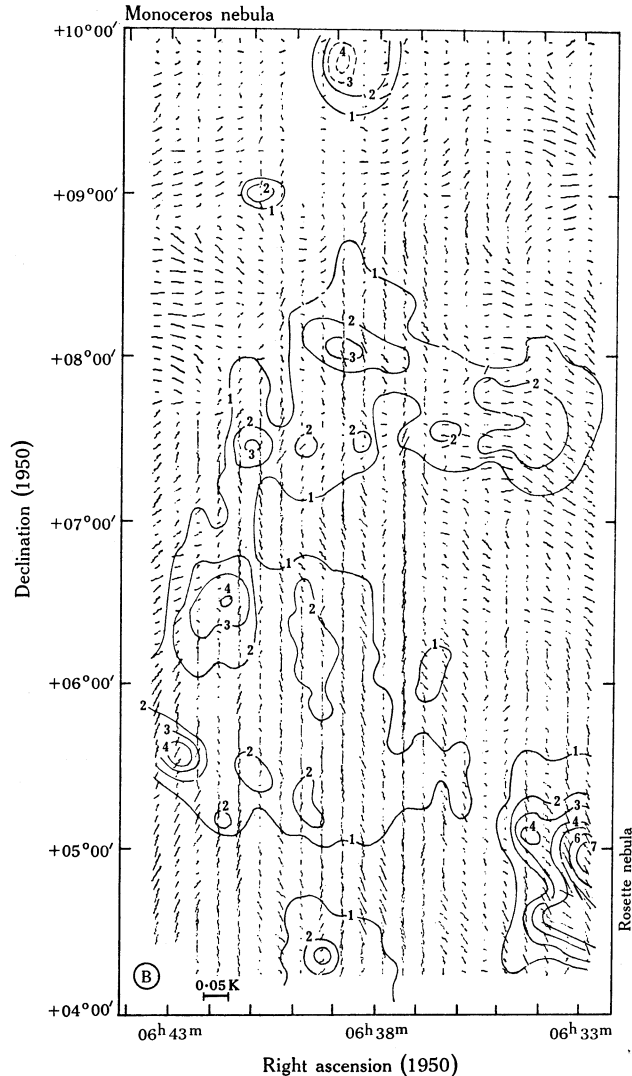
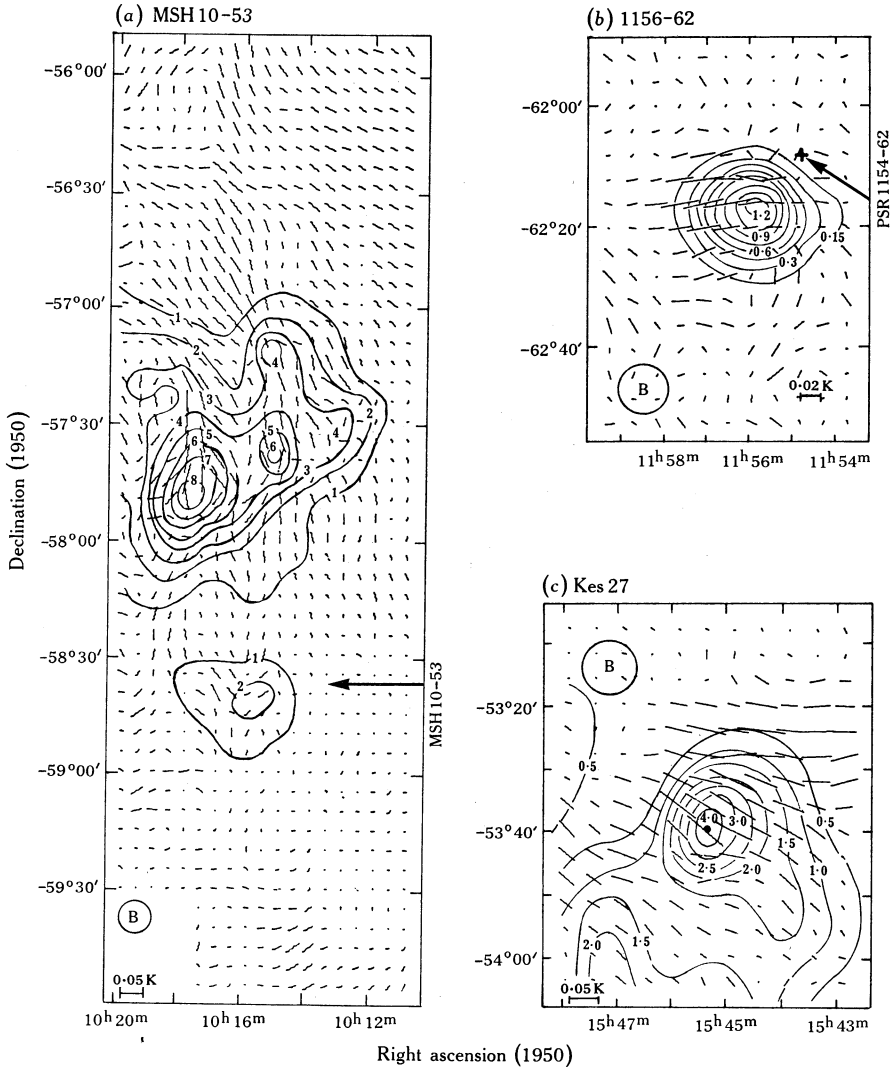


Fig. 3. Total-power contours and polarization  $E$  vectors at 2700 MHz for the Monoceros nebula. The contour unit is 0.05 K, and the  $E$  vector scale and beam (B) are given.

1156-62, G296.8-0.3

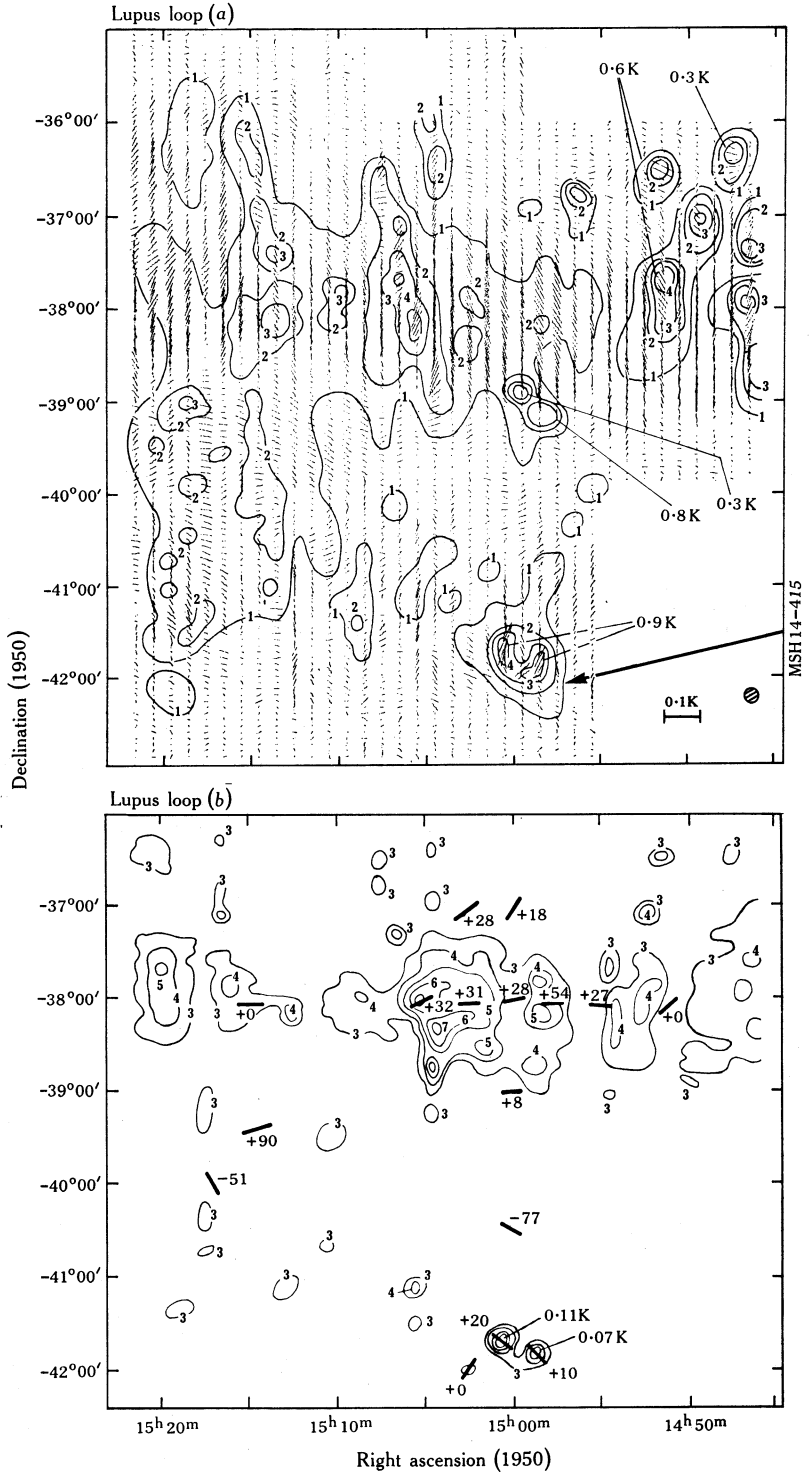
Large and Vaughan (1972) suggested that 1156-62 is a supernova remnant and that it might be associated with the nearby pulsar PSR 1154-62. Our resolution is considerably worse than theirs, and in Fig. 4b we do not resolve the characteristic

SNR structure seen in Large and Vaughan's 408 MHz isotherms. The bulge in the lower brightness contours on the western side of the source suggests the presence of a confusing source, which presumably is thermal. There appears to be polarization, in excess of 5%, associated with 1156-62. The present flux density (4.7 f.u.) is consistent with the values quoted by Large and Vaughan for a spectral index of  $-0.7$ .



**Fig. 4.** Total-power contours and polarization  $E$  vectors at 2700 MHz for (a) MSH 10-53, (b) 1156-62 and (c) Kes 27. The contour unit is 1.0 K, and the  $E$  vector scale and beam (B) are given.

**Fig. 5.** Polarization results at 2700 MHz for the Lupus loop, with some peak temperatures indicated: (a) Total-power contours and polarization  $E$  vectors. The contour unit is 0.05 K, and the  $E$  vector scale and the beam (hatched ellipse) are given. (b) Contours of polarization brightness temperature. The contour unit is 0.01 K, and directions of the projected magnetic field and values of the rotation measure ( $\text{rad m}^{-2}$ ) are indicated.



*Kes 27, G327.4+0.4*

There seems to be a considerable degree of polarization associated with the SNR Kes 27, both at 2700 MHz (Fig. 4c) and at 5000 MHz (as shown by our unpublished 5000 MHz data). The percentage polarization averages  $\sim 2\%$  over the source but rises considerably around the northern side.

*Lupus Loop, G330.0+15.0*

The Lupus loop is a large arc of emission of low surface brightness discovered by Milne (1971*b*) in the vicinity of the supernova of 1006 AD. The remnant of SN 1006 AD is well identified with the smaller-diameter shell source MSH 14-415 (Gardner and Milne 1965) and is not considered to be in any way associated with the Lupus loop.

Observations of the Lupus loop were difficult to make because of its low surface brightness and large angular size. The scan spacing in right ascension was much coarser than desired. However, the polarization in the vicinity of the source is remarkably intense and uniform over large areas, and Fig. 5*a* shows satisfactorily the broad features of the polarization and total-power distribution. The degree of polarization is seen to be well related to the total-power isotherms, and this is better illustrated in Fig. 5*b*, where the isotherms of polarization temperature are shown. Some of the knots of polarization seen in the westernmost scans are in the direction of sources believed by Milne (1971*b*) to be extragalactic field sources. The polarization associated with MSH 14-415 (SN 1006 AD) agrees well with Milne's more detailed 2700 MHz map of this source.

From the present 2700 MHz data and those at 1660 and 1410 MHz (Milne 1971*b*), it is possible to deduce a direction for the magnetic field in a few areas where the polarization is uniform at the three frequencies. The requirement of uniformity stems from the existence of three different resolutions. The resulting magnetic field directions and rotation measures are shown in Fig. 5*b*. The rotation measures are relatively small, being  $\sim +30 \text{ rad m}^{-2}$  in the strongly polarized region centred on R.A.  $15^{\text{h}}00^{\text{m}}$ , Dec.  $-38^\circ$ , and becoming negative to the south or east. However, these conclusions are very uncertain and more data at other frequencies are required. The flux density measured here, together with the values given by Milne suggests a spectral index of  $-0.5$  for the Lupus loop.

*Kes 40, G337.3+1.0*

There is considerable polarization in the direction of Kes 40. However, the most intense polarization in Fig. 6*a* is in the south-western corner, away from the radio source, so that association between this polarization and the SNR is doubtful. There is a decrease in the polarized intensity in the direction of Kes 40, which suggests that there is polarization associated with the SNR at position angles opposing the general background polarization. The flux density (8 f.u.) measured here is 50% higher than the value of 5 f.u. obtained by Thomas and Day (1969).

*MSH 17-39, G357.7-0.1*

The source (Fig. 6*b*) was scanned in right ascension rather than declination. There is an increase in the polarization intensity in the direction of the source, but the effect is barely above the noise level.

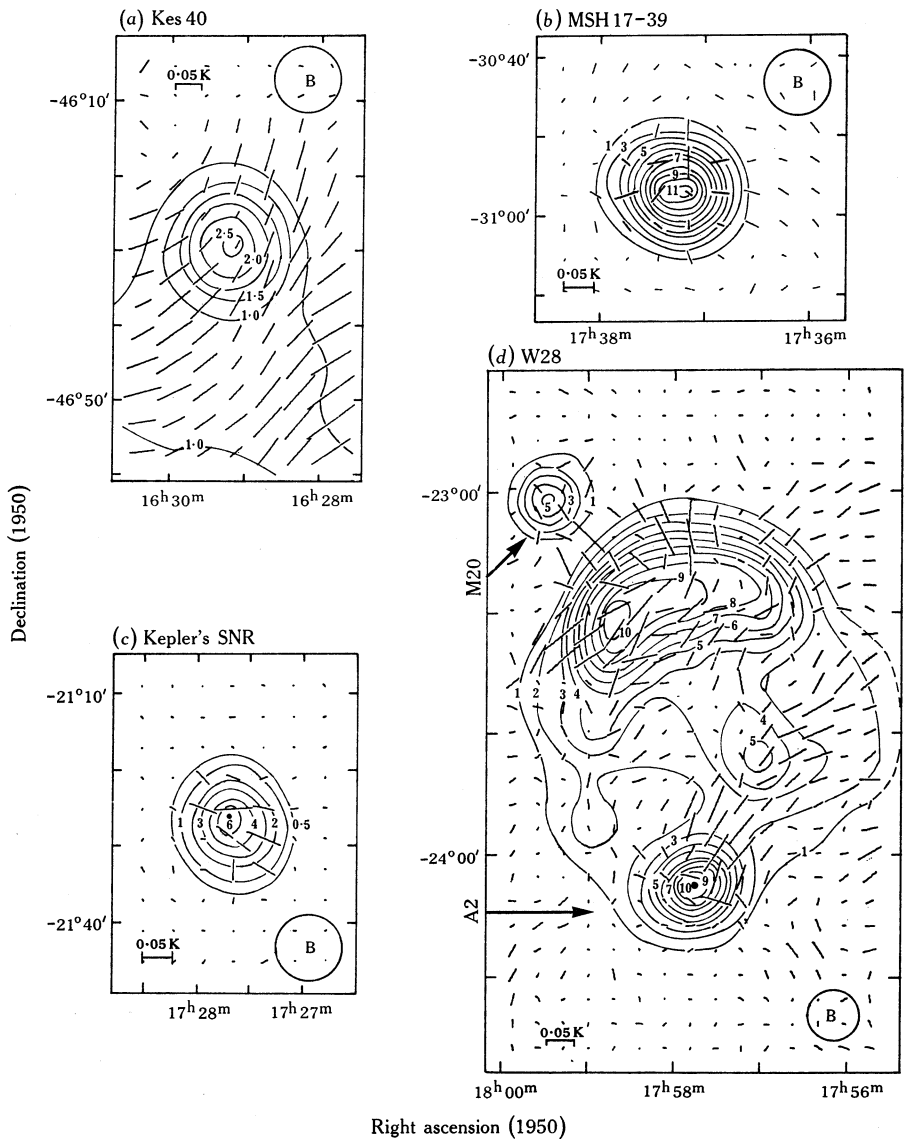


Fig. 6. Total-power contours and polarization  $E$  vectors at 2700 MHz for (a) Kes 40, (b) MSH 17–39, (c) Kepler's SNR and (d) W28. The contour unit is 1.0 K, and the  $E$  vector scale and beam (B) are given.

#### *Kepler's SNR, $G4.5+6.8$*

The present flux density (9 f.u.) for Kepler's SNR is perhaps a little lower than is expected from the published spectra (e.g. Milne 1969). The polarization shown in Fig. 6c is confined to the source and amounts to 1%–2% of the total-power intensity.

#### *W28, $G6.4-0.1$*

There is reasonable agreement between the present polarization  $E$  vectors for W28 and those obtained in the restricted surveys of Kundu and Velusamy (1970)

and Milne and Wilson (1971). The most northern and the most southern sources in Fig. 6*d*, M20 and A2 respectively, are both thermal, and their flux densities are given separately in Table 1.

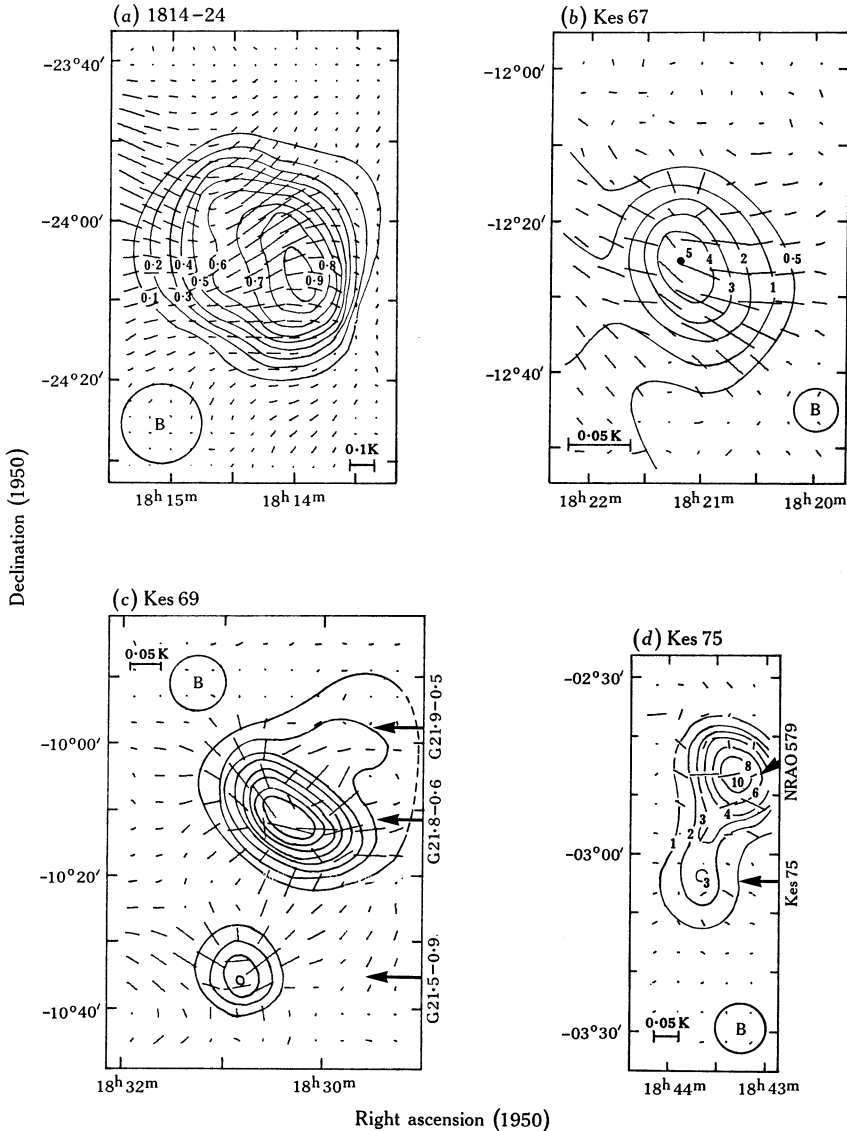


Fig. 7. Total-power contours and polarization  $E$  vectors at 2700 MHz for (a) PKS 1814–24, (b) Kes 67, (c) Kes 69 and (d) Kes 75. The contour unit is 1.0 K, and the  $E$  vector scale and beam (B) are given.

#### PKS 1814–24, G7.7–3.7

This extended source was found to be highly polarized at 5000 MHz by Gardner *et al.* (1969). Integrated flux densities have been measured at four other frequencies by one of us (D.K.M., unpublished data):  $13 \pm 1.5$  f.u. at 408 MHz,  $11.3 \pm 1.0$  f.u.

at 635 MHz,  $8.35 \pm 1.0$  f.u. at 1410 MHz and  $7.7 \pm 1.0$  f.u. at 2650 MHz. These, together with the 2700 MHz value given in Table 1, yield a nonthermal spectral index of  $-0.36$ . The source is possibly the same as MSH 18-25 which Mills *et al.* (1960) list at the same declination but  $19'$  arc to the west. (A search by D.K.M did not yield any likely source nearer than this to the position of MSH 18-25.) However, the 86 MHz flux density (71 f.u.) of MSH 18-25 is much greater than expected from the spectrum for PKS 1814-24. With such a large angular size ( $\sim 23' \times 17'$  arc) and a nonthermal spectrum, this object is undoubtedly an SNR. The polarization in Fig. 7a is seen to extend well beyond PKS 1814-24 but it is most intense on the source, where it is  $\sim 10\%$  of the total intensity.

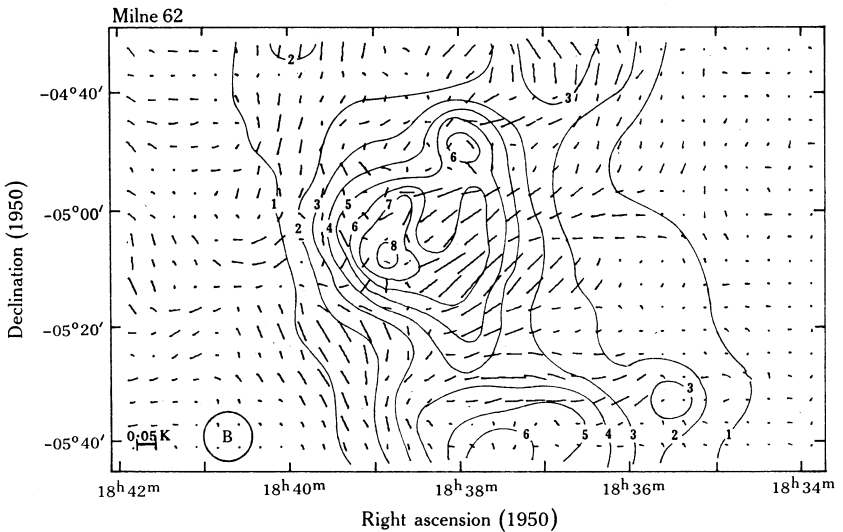


Fig. 8. Total-power contours and polarization  $E$  vectors at 2700 MHz for Milne 62. The contour unit is  $1.0$  K, and the  $E$  vector scale and beam (B) are given.

### *Kes 67, G18.9+0.3*

The intense uniform polarization passing through Kes 67, MSH 18-18 (Fig. 7b), suggests that it is associated with this source. The percentage polarization is between  $1\%$  and  $2\%$  over the source. At higher resolutions (Kesteven 1968; Milne 1969) this source is seen to have a partial shell structure somewhat similar to W44, which also exhibits fairly uniform polarization directions throughout (see below).

### *Kes 69, G21.8-0.5*

The source Kes 69, MSH 18-113, is a nonthermal source with a diameter of about  $20'$  arc. At higher resolutions (e.g. Shaver and Goss 1970) there is a well-defined shell structure outlined in Fig. 7c by the strong source G21.8-0.6 and the weaker G21.9-0.5 to the north-west. The additional source G21.5-0.9 shown in this figure has a flat spectrum between 1660 and 5000 MHz so that the polarization seemingly associated with this source may be associated with the background. It is evident from Fig. 7c that Kes 69 is strongly polarized and this is even more clearly

established from our unpublished 5000 MHz results. The percentage polarization in Fig. 7c varies between 1% and 3% over Kes 69.

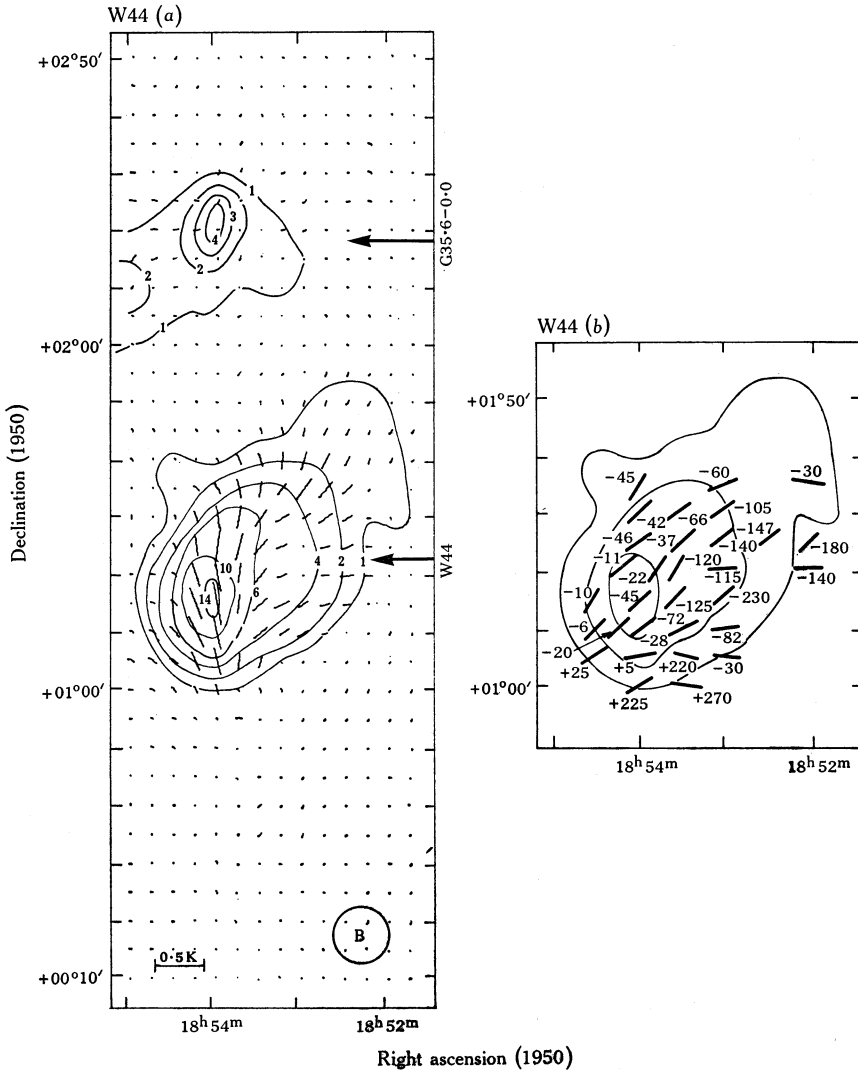


Fig. 9. Polarization results at 2700 MHz for W44: (a) Total-power contours and polarization  $E$  vectors. The contour unit is 1.0 K, and the  $E$  vector scale and the beam (B) are given. (b) Directions of the projected magnetic field and values of the rotation measure ( $\text{rad m}^{-2}$ ).

#### Kes 75, G29.7-0.2

The source Kes 75 is the low-level extension to the south of the strong thermal source NRAO 579 which dominates Fig. 7d. There is evidently no polarization associated with Kes 75; the increased polarization temperature on NRAO 579 is only the residual polarization after considerable spurious polarization (due mainly to the gradient effect) was removed (cf. the residual polarization on Hydra A in Fig. 1).

*Milne 62, G27.3+0.0*

This region was scanned in right ascension. The source suggested by Milne (1969) as an SNR is a loop 32' arc in diameter centred on R.A. 18<sup>h</sup> 38<sup>m</sup> 30<sup>s</sup>, Dec. -05° 05' (1950) containing the small-diameter sources Kes 73 and 3C 387. It would be difficult to claim a positive link between the polarization shown in Fig. 8 and Milne 62, although the polarization is most intense on and near this source. The percentage polarization over the source has an average value of only 1%. From the value for the flux density obtained here together with the values given by Willis (1972), a spectral index of -0.53 is obtained. However, the region is quite complex and contains at least one thermal source (Milne 1969; Willis 1972).

*W44, G34.6-0.5*

The polarization observations of W44 presented in Fig. 9a provide a third frequency to complement the observations at 10 800 MHz (3' arc resolution) and 5000 MHz (6' arc) (Kundu and Velusamy 1969, 1972) and at 5000 MHz (4' arc) (Whiteoak and Gardner 1971). From their 10 800 and 5000 MHz polarization distributions, Kundu and Velusamy (1972) have deduced the directions of the projected magnetic field and the distribution of Faraday rotation measure over W44. The present observations provide a third frequency in this analysis and essentially confirm Kundu and Velusamy's conclusion except on the eastern side of W44, where they obtained positive values for the rotation measure, while we obtain negative values. The direction of the projected magnetic field and values of the rotation measure presented in Fig. 9b are deduced from the 2700 and 5000 MHz data, with the 10 800 MHz data of Kundu and Velusamy used to remove uncertainties arising from the 180° ambiguity in the observed position angles. The source G35.6-0.0 seen in Fig. 9a to the north of W44 was thought to be nonthermal ( $\alpha = -0.5$ ; Altenhoff *et al.* 1970). However, the discovery of an H109 $\alpha$  recombination line in this direction (Dickel and Milne 1973), together with recent high-resolution continuum observations at 408 and 5000 MHz (J. L. Caswell and D. H. Clark, personal communication), now suggests that G35.6-0.0 is an HII region.

## Conclusions

It is clear from the present observations and those of Milne (1972) that, except for the brightest SNRs, the background polarization and the polarization associated with the SNRs are of similar magnitudes, so that maps of the SNR polarization must include sufficient of this background to assess its effect.

## References

- Altenhoff, W. J., Downes, D., Goad, L., Maxwell, A., and Rinehart, R. (1970). *Astr. Astrophys. Suppl. Ser.* **1**, 319.  
Caswell, J. L. (1970). *Aust. J. Phys.* **23**, 105.  
Davies, R. D. (1963). *Observatory* **83**, 172.  
Day, G. A., Caswell, J. L., and Cooke, D. J. (1972). *Aust. J. Phys.* **25**, 1.  
Dickel, J. R., and Milne, D. K. (1973). *Aust. J. Phys.* **26**, 267.  
Gardner, F. F., and Milne, D. K. (1965). *Astr. J.* **70**, 754.  
Gardner, F. F., Whiteoak, J. B., and Morris, D. (1969). *Aust. J. Phys.* **22**, 821.  
Haslam, C. G. T., and Salter, C. J. (1971). *Mon. Not. R. astr. Soc.* **151**, 385.

- Kesteven, M. J. L. (1968). *Aust. J. Phys.* **21**, 739.
- Kundu, M. R., and Velusamy, T. (1969). *Astrophys. J.* **155**, 807.
- Kundu, M. R., and Velusamy, T. (1970). *Astrophys. J.* **162**, 17.
- Kundu, M. R., and Velusamy, T. (1972). *Astr. Astrophys.* **20**, 237.
- Large, M. I., and Vaughan, A. E. (1972). *Nature Phys. Sci.* **236**, 117.
- Lozinskaya, T. A. (1972). *Soviet Astr. AJ* **15**, 910.
- Mills, B. Y., Slec, O. B., and Hill, E. R. (1960). *Aust. J. Phys.* **13**, 676.
- Milne, D. K. (1969). *Aust. J. Phys.* **22**, 613.
- Milne, D. K. (1971a). *Aust. J. Phys.* **24**, 429.
- Milne, D. K. (1971b). *Aust. J. Phys.* **24**, 757.
- Milne, D. K. (1972). *Aust. J. Phys.* **25**, 307.
- Milne, D. K., and Dickel, J. R. (1971). *Nature* **231**, 33.
- Milne, D. K., and Hill, E. R. (1969). *Aust. J. Phys.* **22**, 211.
- Milne, D. K., and Wilson, T. L. (1971). *Astr. Astrophys.* **10**, 220.
- Shaver, P. A., and Goss, W. M. (1970). *Aust. J. Phys. astrophys. Suppl.* No. 14, 77.
- Thomas, B. MacA., and Day, G. A. (1969). *Aust. J. Phys. astrophys. Suppl.* No. 11, 19.
- Whiteoak, J. B., and Gardner, F. F. (1971). *Aust. J. Phys.* **24**, 913.
- Willis, A. G. (1972). Ph.D. Thesis, University of Illinois.

Manuscript received 14 January 1974